Lattice-fringe fingerprinting of an iron-oxide nanocrystal supported by an open-access database

Peter Moeck[1°], Ruben Bjorge[1], Eric Mandell[2], and Philip Fraundorf[2,3]
[1] Nanocrystallography Group, Department of Physics, Portland State University, P.O. Box 751, Portland, OR 97207-0751, U.S.A.; [°] Oregon Nanoscience and Microtechnologies Institute, http://www.onami.us
[2] Department of Physics and Astronomy & [3] Center for Molecular Electronics, University of Missouri at St. Louis, MO 53121, U.S.A.

ABSTRACT

Lattice-fringe fingerprinting in two dimensions (2D) is demonstrated for a nanocrystal from a mixture of magnetite and maghemite. The mainly inorganic subset of the Crystallography Open Database (COD) provides the theoretical lattice-fringe fingerprints that are needed for the identification of the crystal phase.

Keywords: nanocrystals, crystal phase, databases, electron microscopy

INTRODUCTION

For a variety of reasons, see. e.g. [1], a "whole new crystallographic world" is waiting to be discovered in the nanocrystal realm. To aid such discoveries image-based nanocrystallography in high-resolution phase contrast transmission electron microscopy (HRTEM) [1-8] and atomic resolution scanning transmission electron microscopy (STEM) [9] have been proposed. Lattice-fringe fingerprinting in two (2D) [1-5] and three (3D) dimensions [2,6-8] are straightforward applications of such image-based nanocrystallography techniques.

STEM images typically show scan aberration artifacts such as distortions in the resolved spatial frequencies, resulting in distortions in the angles between lattice fringes. These distortions can, in principle, be corrected for each individual STEM operated under its typical imaging conditions [10]. Lens aberration corrected TEMs, e.g. [11], allow for sufficiently thin crystals the retrieval of the Fourier coefficients of the projected electrostatic potential at the sub-Ångström length scale and represent a novel type of crystallographic instrument in support of both electron crystallography [12,13] and image-based nanocrystallography [1-8]. The enhanced viability of image-based nanocrystallography in such microscopes has been illustrated by model calculations [6,7].

Enabled and encouraged by the Crystallographic Information File (CIF) [14-16] standard of the International Union of Crystallography, members of the international crystallographic community are developing open-access databases [17-20]. The Crystallography Open Database (COD) [17,18] is the result of such efforts. It is growing rapidly and currently comprises more than 50,000 entries.

There are, thus, complementary developments by different communities to address structural questions within the nanocrystal realm. In order to contribute to these developments and to promote lattice-fringe fingerprinting in 2D [1-5], we will identify in this paper the crystal phase of an individual nanocrystal from a mixture of nanocrystalline magnetite (Fe_3O_4, space group: $Fd\bar{3}m$, origin at $\bar{4}3m$), a = 0.832 nm, [21]) and maghemite. The latter is an important material for the magnetic recording and magnetic fluids industries [22,23] (as well as a topotactic oxidation product of magnetite).

Depending on the statistically ordered distribution of iron vacancies within the spinel prototype, maghemite (?-Fe_2O_3) crystallizes either in space group $P4_132$ or $P4_32_12$. While the above mentioned cubic crystal phase of maghemite possesses a lattice constant of 0.833 nm, one of the three lattice parameters is trice as long in the tetragonal crystal phase [22]. There is also a quasi-hypothetical cubic maghemite phase with space group $Fd\bar{3}m$, (origin at the center, $\bar{3}m$), with a = 0.833 nm [22]. The iron vacancies within the spinel prototype are in that crystal phase randomly distributed, but such a distribution seems to be seldom realized [22].

The relative phase contents of mixtures of magnetite and maghemite nanocrystals are almost impossible to quantify by standard laboratory based powder X-ray diffraction techniques because these iron oxide phases can form metastable solid solutions and their lattice constant are rather similar. In addition, the average grain size in our sample is on the order of a few tens of nm. For the effect of average grain size of maghemite nanocrystals on powder X-ray (Cu-K_a) diffraction pattern see, e.g. [23]. It is interesting to note that while grain sizes of tens of nm to a few nm make powder X-ray diffraction less useful to useless for crystal phase identification, they have exactly the opposite effect on the feasibility of lattice-fringe fingerprinting of nanocrystals because lattice fringes become visible over a wider angular range [2].

The phase content of our magnetite/maghemite mixtures can, therefore, in principle, be quantified on the basis of lattice-fringe fingerprinting in 2D. A representative number of individual nanocrystals would need to be processed and for that to be practical, the method would need to be automated. Such automation is, however, technically feasible with the current generation of computer controlled TEMs.

It has been known for more than a quarter of a century that lattice parameters can be derived from lattice fringes with an accuracy of up to about 0.01 % [24-26] (where axial imaging conditions need to be employed [27]). Obtainable statistical precisions are for lattice constants on the order of 0.2 % [26] and for the (intersecting) angles between reciprocal lattice vectors (net-plane normals) on the order of 0.2 ° [25].

The lattice constants of nanocrystals with diameters between ten and one nm, on the other hand, may be contracted (or expanded) by a fraction of a percent, e.g. [23], up to a few percent at worst (for the very smallest crystals) due to free-energy minimization effects in the presence of a large surface areas [28]. It is also known that many nanocrystals possess surface and near surface areas that are highly distorted with respect to the bulk crystal structure. Anatase nanocrystals of less than about 2 nm may, for example, not possess a core region that corresponds to the bulk lattice structure [29]. For our method to be practical, the nanocrystals should, therefore, be on the order of a few to a few tens of nanometers.

LATTICE-FRINGE FINGERPRINTING PROCEDURE

HRTEM images, e.g., Fig. 1a were recorded from our magnetite/maghemite sample (with a magnification of 240,000 times) at a Philips EM 430ST operated at 300 kV [30]. The point resolution of this microscope is 0.19 nm. In other words, information in reciprocal space out to 5.26 nm^{-1} is for this microscope directly interpretable in the weak-phase object/kinematic approximation when images are recorded at the Scherzer (de)focus.

The images were digitized (at 2400 pixels per inch [30]) and convoluted with a Hanning window [3] in order to reduce streaking in the subsequent calculation of a Fourier transform employing Gatan's Digital Micrograph software. The inverted Fourier transform power spectrum of Fig. 1a is displayed as Fig. 1b.

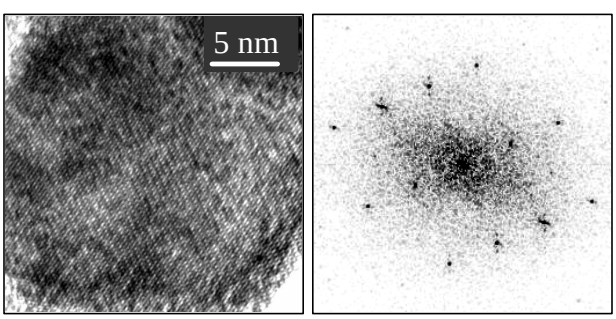

Figure 1: HRTEM data from an iron-oxide nanocrystal (a) image as obtained, (b) processed image.

Employing a scripted user-written program [3] in Digital Micrograph and the formulae given in ref. [31] for sub-pixel interpolation, the length of reciprocal lattice vectors and their intersecting angles were derived. The experimental lattice-fringe fingerprint plot, Fig. 2, was derived from these data. There is a one-to-one correspondence of the location of the data points in Fig. 2 and the circled data points in the theoretical lattice-fringe fingerprint plot for magnetite (in the kinematic limit), Fig. 3. No such correspondence between experimentally derived data and predicted data exists for either one of the theoretical lattice-fringe fingerprint plots of the "vacancy ordered maghemites" (in the kinematic limit).

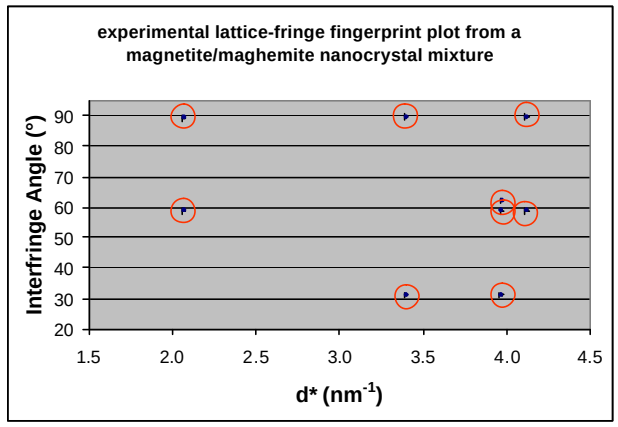

Figure 2: Experimental lattice-fringe fingerprint plot (intersecting angle versus spatial frequency of lattice fringes). Data points with spatial frequency higher than that of the microscope's point resolution are omitted.

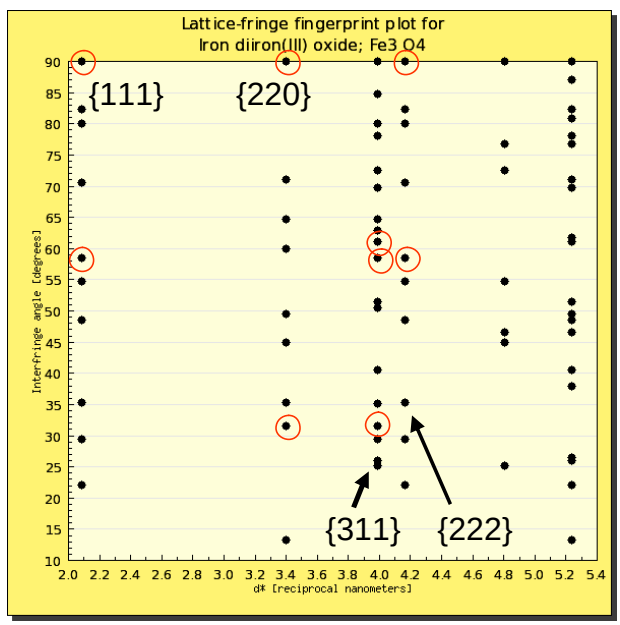

Figure 3: Theoretical lattice-fringe fingerprint plot of magnetite (in the kinematical limit) on that basis of the data in ref. [21]. The data points that match their experimental counterparts in Fig. 2 are circled. The families of reciprocal lattice vectors (net planes) that correspond to these data points are labeled.

The theoretical lattice-fringe fingerprint plots were calculated on-line from CIFs that are part of the mainly

inorganic subset [19,20] of the COD [17,18]. Approximately 10,500 CIFs, their three-dimensional visualization, and corresponding theoretical lattice fringe fingerprints are accessible freely over the internet from this subset [19], Fig. 4. For candidate structures, searches can be performed with Boolean constraints for elements absent and/or present and the strict number of elements present.

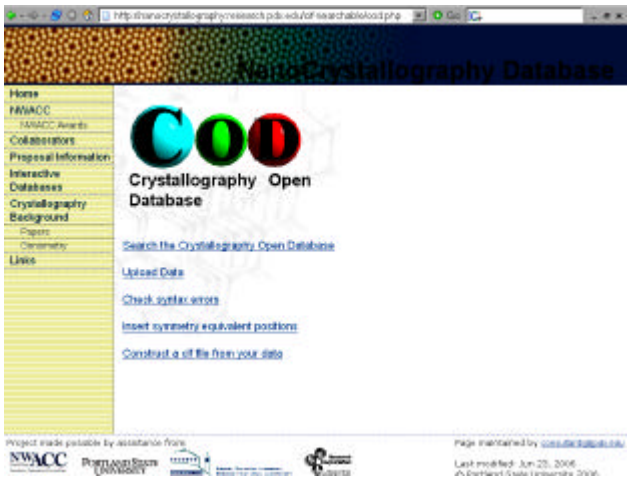

Figure 4: Home page of the mainly inorganic subset [19,20] of the COD [17,18].

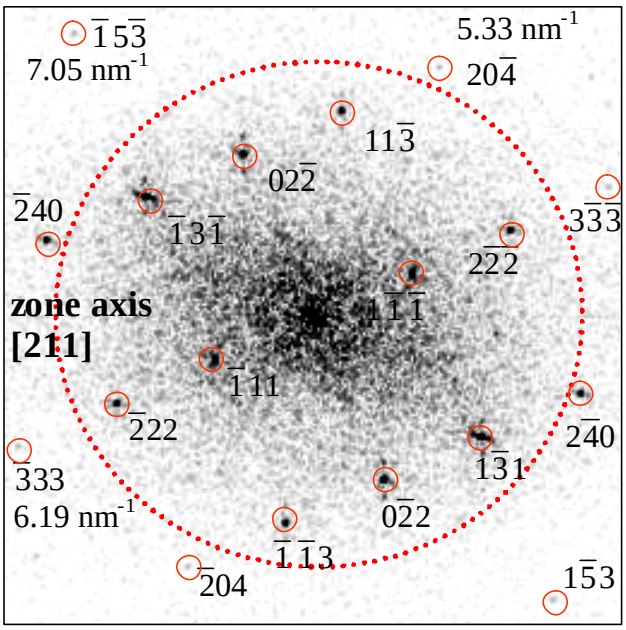

Figure 5: Indexed Fourier transform power spectrum of the HRTEM image in Fig. 1a. The microscope's point resolution, 0.526 nm^{-1}, is marked approximately by the dotted circle. Spatial frequencies beyond this limit are given next to the respective spot's label.

After the identification of the crystal phase from a range of candidates, the Fourier transform power spectrum of a nanocrystal can be indexed, Fig. 5. The Fourier transform of the HRTEM image can also be scrutinized more thoroughly to ensure that the crystal phase identification has been correct and unambiguous.

Within the weak-phase object/kinematic approximation, the latter can be done by an extraction of the Fourier coefficients of the projected electrostatic potential [12]. Note that these coefficients are directly proportional to the crystallographic structure factors, which in turn depend on the atomic arrangement within the unit cells and can be calculated from the CIFs of the mainly inorganic subset [19,20] of the COD [17,18]. In addition, there is always the possibility of complementing the information that was extracted in 2D with information that is gathered by image-based nanocrystallography in 3D [2,6-8].

SUMMARY AND CONCLUSIONS

Lattice-fringe fingerprinting for the identification of the crystal phase of a nanocrystal has been demonstrated on a sample with industrial relevance. An open-access database that supports this method was also mentioned.

Because the presented analysis has been done only at the lattice geometry and kinematic extinctions levels, an unambiguous distinction between a nanocrystal of the magnetite phase and one of the above mentioned quasi-hypothetical cubic maghemite (with the same space group and almost the same lattice constant) cannot be made. It might, however, be possible that the extracted Fourier coefficients of the projected electrostatic potential are for both crystal phases sufficiently different to allow such a distinction.

We conclude that our method is entirely feasible and also amendable to automation. When automated, the crystal phase content of mixtures of nanocrystals can be analyzed both qualitatively and quantitatively.

ACKNOWLEDGMENTS

This research was supported by an award from Research Corporation. The creation of the web sites that house our mainly inorganic subset of the COD was sponsored by the NorthWest Academic Computing Consortium. Support was also provided by the Oregon Nanoscience and Microtechnologies Institute (ONAMI) and an Internationalization Award from Portland State University (PSU). We are grateful to Dr. Bjoern Seipel (PSU) and Ján Zahornadský (Charles University of Prague) for writing software that calculates theoretical lattice-fringe fingerprint plots. Dr. Klaus H. Pecher from the Pacific Northwest National Laboratory is thanked for the sample. William Garrick (PSU) is thanked for managing the research servers that host our databases.

REFERENCES

[1] P. Moeck, J. Zahornadský, B. Dušek, and P. Fraundorf, "Image-based Nanocrystallography with on-line Database Support", *Proc. of SPIE* Vol. **6370**, paper 6370-48, October 1-4, 2006, eds. N.K. Dhar, A.K. Dutta, and M. Islam.

[2] P. Fraundorf, W. Qin, P. Moeck, and E. Mandell, "Making sense of nanocrystal lattice fringes", *J. Appl. Phys*. **98** (2005) 114308-1-114308-10; *arXiv:cond-mat/0212281 v2*; *Virtual Journal of Nanoscale Science and Technology* Vol. **12** (2005) Issue 25.
[3] R. Bjorge, *MSc thesis*, Department of Physics, Portland State University, 2007, in preparation
[4] P. Moeck, B. Seipel, R. Bjorge, and P. Fraundorf, "Lattice fringe fingerprinting in two dimensions with database support", *NSTI-Nanotech 2006*, Vol. **1** (2006) 741-744.
[5] P. Moeck, O. Certík, B. Seipel, R. Groebner, L. Noice, G. Upreti, P. Fraundorf, R. Erni, N. D. Browning, A. Kiesow, and J.-P. Jolivet, "Identifying unknown nanocrystals by fringe fingerprinting in two dimensions & free-access crystallographic databases", *Two- and Three-Dimensional Methods for Inspection and Metrology III*, edited by K.G. Harding, *Proc. of SPIE*, Vol. **6000** (2005) 60000M-1-60000M-12.
[6] P. Moeck and P. Fraundorf, "Transmission electron goniometry and its relation to electron tomography for materials science applications", *arXiv:cond-mat/06113454 v2*.
[7] P. Moeck, W. Qin, and P. Fraundorf, "Image-based Nanocrystallography by means of Transmission Electron Goniometry", *Nonlinear Analysis* **63** (2005) e1323-e1331.
[8] W. Qin and P. Fraundorf, "Lattice parameters from direct-space images at two tilts", *Ultramicroscopy* **94** (2003) 245-262; *arXiv:cond-mat/0001139*.
[9] P. Wang, A.L. Bleloch, U. Falke, and P.J. Goodhew, "Geometric aspects of lattice contrast visibility in nanocrystalline materials using HAADF STEM", *Ultramicroscopy* **106** (2006) 277-283.
[10] A.M. Sanchez, P.L. Galindo, S. Kret, M. Falke, R. Beanland, and P. J. Goodhew, "An approach to the systematic distortion correction in aberration-corrected HAADF images", *J. Microsc.* **221** (2006) 1-7.
[11] S.J. Pennycook, M. Varela, C.J.D. Hetherington, and A.I. Kirkland, "Materials Advances through Aberration-Corrected Electron Microscopy", *MRS Bulletin* **31** (January 2006) 36-43.
[12] S. Hovmöller, X.D. Zuo, and T.E. Weirich, "Crystal Structure Determination from EM Images and Electron Diffraction Patterns", in *Advances in Imaging and Electron Physics: Microscopy, Spectroscopy, Holography and Crystallography with Electrons*, Vol. **123** (2002) 257-289, editors: P.E. Hawkes, B. Kazan, and T. Mulvey.
[13] D.L. Dorset, "Correlations, convolutions and the validity of electron crystallography", *Z. Kristallogr*. **218** (2003) 237-246.
[14] http://www.iucr.org/iucr-top/cif/index.html.
[15] I.D. Brown and B. McMahon, "CIF: the computer language of crystallography", *Acta Cryst. B* **58** (2002) 317-324.
[16] S. Hall and B. McMahon (editors), *International Tables for Crystallography, Vol. **G**: Definition and exchange of crystallographic data*, Chester, International Union of Crystallography, 2005, see http://it.iucr.org/.
[17] http://crystallography.net.
[18] M. Leslie (editor), "Free the Crystals", *Science* **310** (2005) 597; D. Chateigner et al., "COD (Crystallography Open Database) and PCOD (Predicted)", *XXth Congress of the International Union of Crystallography (IUCr)*, Florence (Italy), August 23-31, 2005; A. Le Bail, "Does open data better serve the crystallographic community?" *International Union of Crystallography Newsletter* **12**(2) (2004) 27, www.iucr.org, ISSN 1067-0696.
[19] http://nanocrystallography.research.pdx.edu.
[20] P. Moeck and P. Fraundorf, "Freely Accessible Crystallographic Internet Resources for Materials Science Research and Education", *Materials Science and Technology (MS&T) 2006*: Fundamentals and Characterization, Vol. **1**, 119-128.
[21] W.H. Bragg, "The Structure of Magnetite and the Spinels", Nature (London) **95** (1915) 561-574.
[22] C. Pecharroman, T. Gonzalez-Carreno, and J.E. Iglesias, "The infrared dielectric properties of maghemite, gamma-Fe_2O_3, from reflectance measurement on pressed powders", *Physics and Chemistry of Minerals* **22** (1995) 21-29.
[23] J.A. López-Pérez, M. A. López Quintela, J. Mira, J. Rivas, and S.W. Charles, "Advances in the Preparation of Magnetic Nanoparticles by the Microemulsion Method", *J. Phys. Chem. B* **101** (1997) 8045-8047.
[24] P.G. Self, H.K.D.H. Bhadeshia, and W.M. Stobbs, "Lattice spacings from lattice fringes", *Ultramicroscopy* **6** (1981) 29-40.
[25] W.J. de Ruijter, R. Sharma, M.R. McCartney, and D.J. Smith, "Measurement of lattice-fringe vectors from digital HREM images: experimental precision", *Ultramicroscopy* **57** (1995) 409-422.
[26] J. Biskupek and U. Kaiser, "Practical considerations on the determination of the accuracy of the lattice parameter measurements from digital recorded diffractograms", *J. Electron. Microsc.* **53** (2004) 601-610.
[27] J.G. Allpress, E.A. Hewat, A.F. Moodie, and J.V. Sanders, "n-beam lattice images. I. Experimental and computed images from $W_4Nb_{26}O_{77}$", *Acta Cryst. A* **28** (1972) 528-536.
[28] E. Roduner, *Nanoscopic Materials, Size-dependent Phenomena*, Royal Society of Chemistry, Cambridge, 2006.
[29] J.F. Banfield and H. Zhang, "Nanoparticles in the Environment", in: *Nanoparticles and the Environment*, by J.F. Banfield and A. Navrotsky, *Reviews in Mineralogy & Geochemistry*, Vol. **44**, Mineralogical Society of America, series editor: P.H. Ribbe.
[30] E. Mandell, *PhD thesis*, Department of Physics and Astronomy, University of Missouri, 2007, in preparation.
[31] W.J. de Ruijter, "Determination of lattice parameters from digital micrographs based on measurements in reciprocal space", *J. Comp. Assist. Microsc.* **6** (1994) 195-212.